6520–6529 *Nucleic Acids Research, 2017, Vol. 45, No. 11* *Published online 29 April 2017*
doi: 10.1093/nar/gkx339

Transcriptional mutagenesis reduces splicing fidelity in mammalian cells

João A. Paredes[1], Monika Ezerskyte[1], Matteo Bottai[2] and Kristian Dreij[1,*]

[1]Unit of Biochemical Toxicology, Institute of Environmental Medicine, Karolinska Institutet, 171 77 Stockholm, Sweden and [2]Unit of Biostatistics, Institute of Environmental Medicine, Karolinska Institutet, 171 77 Stockholm, Sweden

Received December 07, 2016; Revised March 13, 2017; Editorial Decision April 14, 2017; Accepted April 18, 2017

ABSTRACT

Splicing fidelity is essential to the maintenance of cellular functions and viability, and mutations or natural variations in pre-mRNA sequences and consequent alteration of splicing have been implicated in the etiology and progression of numerous diseases. The extent to which transcriptional errors or lesion-induced transcriptional mutagenesis (TM) influences splicing fidelity is not currently known. To investigate this, we employed site-specific DNA lesions on the transcribed strand of a minigene splicing reporter in normal mammalian cells. These were the common mutagenic lesions O^6-methylguanine (O^6-meG) and 8-oxoguanine (8-oxoG). The minigene splicing reporters were derived from lamin A (*LMNA*) and proteolipid protein 1 (*PLP1*), both with known links to human diseases that result from deregulated splicing. In cells with active DNA repair, 1–4% misincorporation occurred opposite the lesions, which increased to 20–40% when repair was compromised. Furthermore, our results reveal that TM at a splice site significantly reduces *in vivo* splicing fidelity, thereby changing the relative expression of alternative splicing forms in mammalian cells. These findings suggest that splicing defects caused by transcriptional errors can potentially lead to phenotypic cellular changes and increased susceptibility to the development of disease.

INTRODUCTION

Splicing of pre-mRNA resulting from eukaryotic genes involves specific sequence elements both at the exon–intron boundaries and within introns, including the 5′ and 3′ splice sites preceded by the branch-point sequence and polypyrimidine tract (1). Alternative splicing results in the generation of multiple transcripts from a single gene, thereby expanding the human proteome considerably (2,3). High-throughput sequencing and genome-wide analysis have revealed that >90% of all pre-mRNAs from multi-exon human genes undergo alternative splicing (4,5) and the fidelity and regulation of this process are essential to the control of cellular and organ functions in eukaryotes. Indeed, mutations or natural variations in pre-mRNA sequences that alter splicing have been implicated in the etiology and progression of numerous pathologies, including genetic diseases, neurodegenerative disorders and cancer (6,7).

RNA polymerase II (RNA pol II) plays a central role in the synthesis of pre-mRNA and non-coding RNA in eukaryotic cells (8). Maintenance of the viability of mammalian cells, most of which are quiescent or replicate slowly (9,10), depends strongly on the fidelity of transcription. To ensure a high accuracy fidelity checkpoints are utilized at the steps of insertion, extension and proofreading during the transcriptional elongation of RNA pol II (11). In *Saccharomyces cerevisiae*, several alleles are associated with error-prone transcription and some of these also reduce splicing efficiency and induce phenotypic changes resembling human diseases (12–14). Notably, damaged nucleotides or lesions in DNA can also reduce the fidelity of RNA pol II significantly, thereby introducing transcriptional errors.

Lesion-specific processing of DNA damage by RNA pol II influences RNA synthesis in several ways, causing transcriptional arrest and activating transcription-coupled repair (TCR) or transcriptional bypass, which can potentially result in the incorporation of incorrect bases into nascent RNA, an event referred to as transcriptional mutagenesis (TM) (15–18). The capacity of a DNA lesion to impede transcription depends on several variables, but bulky adducts and distorting DNA cross-links are in general very efficient. Transcriptional bypass of bulky, UV-induced lesions by RNA pol II attenuates activation of TCR, allowing cells to complete ongoing mRNA synthesis and maintain protein homeostasis, thereby promoting resistance to DNA damage and cell survival (19,20). Several commonly occurring, non-bulky DNA lesions, such as O^6-methylguanine (O^6-meG) and 8-oxoguanine (8-oxoG), do not pose a strong hinder to RNA pol II, allowing transcriptional bypass and misincorporation both *in vitro* and *in vivo* (16,17).

*To whom correspondence should be addressed. Tel: +46 8 52487566; Email: kristian.dreij@ki.se

When TM occurs, each round of transcription may produce mRNA with single-base mutations that are translated into a relatively large population of mutated or misfolded proteins with altered functions, sometimes leading to phenotypic changes with significant consequences on cellular regulation (21–25). These altered proteins could also have dominant properties leading to a more prolonged or permanent physiological change (26). Here, we tested the hypothesis that even if a DNA lesion leads to TM which does not alter coding specificity (e.g. intronic mutations, silent mutations), translation might be affected if a regulatory sequence at a splicing site is altered. The capacity of such transcriptional errors to alter splicing fidelity has been proposed before (27), but never examined. To accomplish this, we combined the well-established site-specific positioning of DNA lesions (28) and minigene splice reporters (29) designed to reflect the influence of these mutations on splicing. Our results show that when TM involves a splice site *in vivo*, splicing fidelity is attenuated, thereby altering the relative expression of alternatively spliced forms.

MATERIALS AND METHODS

Construction and modification of minigene splicing reporters

The *LMNA* and *PLP1* minigene splicing reporters were constructed on the basis of previous work (30,31) and adapted to the present study. These reporters were cloned into the pNEW-GFP vector and subsequently modified in order to obtain the following final plasmids: pNEW-LMNA-Rep-GFP WT, pNEW-LMNA-Rep-GFP 1824C>T, pNEW-PLP1-Rep-GFP WT and pNEW-PLP1-Rep-GFP 347C>A. Generation of closed circular vectors containing site-specific base modification (pNEW-LMNA-Rep-GFP O^6-meG and pNEW-PLP1-Rep-GFP 8-oxoG) involved production of ssDNA, *in vitro* synthesis of the complementary strand modified at the specific site, and purification of closed circular dsDNA, as described previously (22,28). All DNA vectors were sequenced for confirmation. For a more detailed description of this procedure, please see the Supplementary data. The splice-site scores were determined by the online Splice-Site Analyzer Tool (http://ibis.tau.ac.il/ssat/SpliceSiteFrame.htm). The sequences of all oligonucleotide primers employed are presented in Supplementary Table S1.

Cell culture and transfection

HEK293 cells were obtained from Dr Katarina Johansson, Department of Medical Biochemistry and Biophysics, Karolinska Institutet and used between passages 6 and 15. Normal human lung WI-38 fibroblasts (ATCC) were used between passages 18 and 25. Primary mouse embryonic fibroblasts (MEFs), both WT and Ogg1 deficient ($OGG1^{-/-}$), were obtained from Dr Pablo Radicella, CEA, France, and used between passages 2 and 4. HEK293 cells were grown in MEM supplemented with 10% FBS, 1 mM sodium pyruvate, non-essential amino acids and penicillin/streptomycin. WI-38 fibroblasts were grown using the same medium, but without non-essential amino acids. MEFs were grown in DMEM/F12 (3:1), supplemented with 10% FBS, 2 mM L-glutamine, 1 mM sodium pyruvate and penicillin/streptomycin. All cells were maintained in a humidified incubator at 37°C and 5% CO_2. HEK293 cells were transfected with Lipofectamine 3000 (Invitrogen) and WI-38 and MEFs were transfected using Nucleofection (Lonza/Amaxa) in accordance with to the manufacturers' protocol. Transfection efficiencies of the LMNA and PLP1 reporter plasmids were approximately 15%, 5% and 25% for the HEK293 cells, WI-38 and MEFs, respectively. In order to block repair of O^6-meG by AGT, 10 μM O^6-bzG (in DMSO, Sigma-Aldrich) was added to the cells 1 h prior to transfection (22). Cells were harvested and analyzed 24 h after transfection.

mRNA sequencing

RNA was purified using the RNeasy mini kit (Qiagen) and then treated with DNase employing TURBO DNA-freeTM (Ambion) according to protocol. cDNA was synthesized using the High-Capacity cDNA Reverse Transcription Kit (Applied Biosystems) and the cDNA from each transfection replicate amplified by PCR with high fidelity Phusion polymerase (Thermo scientific) utilizing specific primers for *LMNA* and *PLP1* (see Supplementary Table S1). The gel-purified PCR products (GeneJet Purification kit, Thermo Scientific) were cloned into a pcDNA3 vector, digested with HindIII–KpnI and subsequently sequenced. In the case of the *LMNA* reporter, 96 individual colonies (24 for each one of the four replicates) were sequenced. With the *PLP1* reporter, pre-screening was performed utilizing tetra-primer ARMS-PCR (32). In brief, colony PCR was performed on 100–150 clones (from four replicates) using the primers as indicated in Supplementary Table S1; the PCR products resolved on a 3% agarose gel as shown in Supplementary Figure S5; and colonies that amplified with the mutant-specific primers propagated for plasmid isolation and subsequent confirmation by sequencing. Differences in levels of TM were analyzed with a two-tailed unpaired t-test ($P < 0.05$) using GraphPad Prism 6.0 software.

Flow cytometry

Cells from at least three independent transfections were harvested, re-suspended in PBS and then immediately analyzed for GFP fluorescence on a BD Accuri C6 Flow Cytometer with a FL-1 filter with 99% attenuation. The GFP-positive cells were gated relative to untransfected cells and all the available measures of GFP fluorescence were included in the analysis. First, the intra-replicate correlation in GFP intensity by combination of experiment and condition was calculated, which showed low levels of correlation (Supplementary Table S2). The observed distribution of GFP signal was markedly right-skewed and thick-tailed. Because of that, $\log_{10}$ transformed median GFP intensities were estimated in the statistical analysis. We used quantile regression with GFP intensity as the dependent variable. The independent variables were the indicator variables for the different conditions and for the different replicates. The WT or O^6-meG condition and the data from the first replicate were left out of the model as reference groups. We estimated the standard errors of the regression coefficients with the robust sandwich estimator (33). For details see Supplementary Table S3.

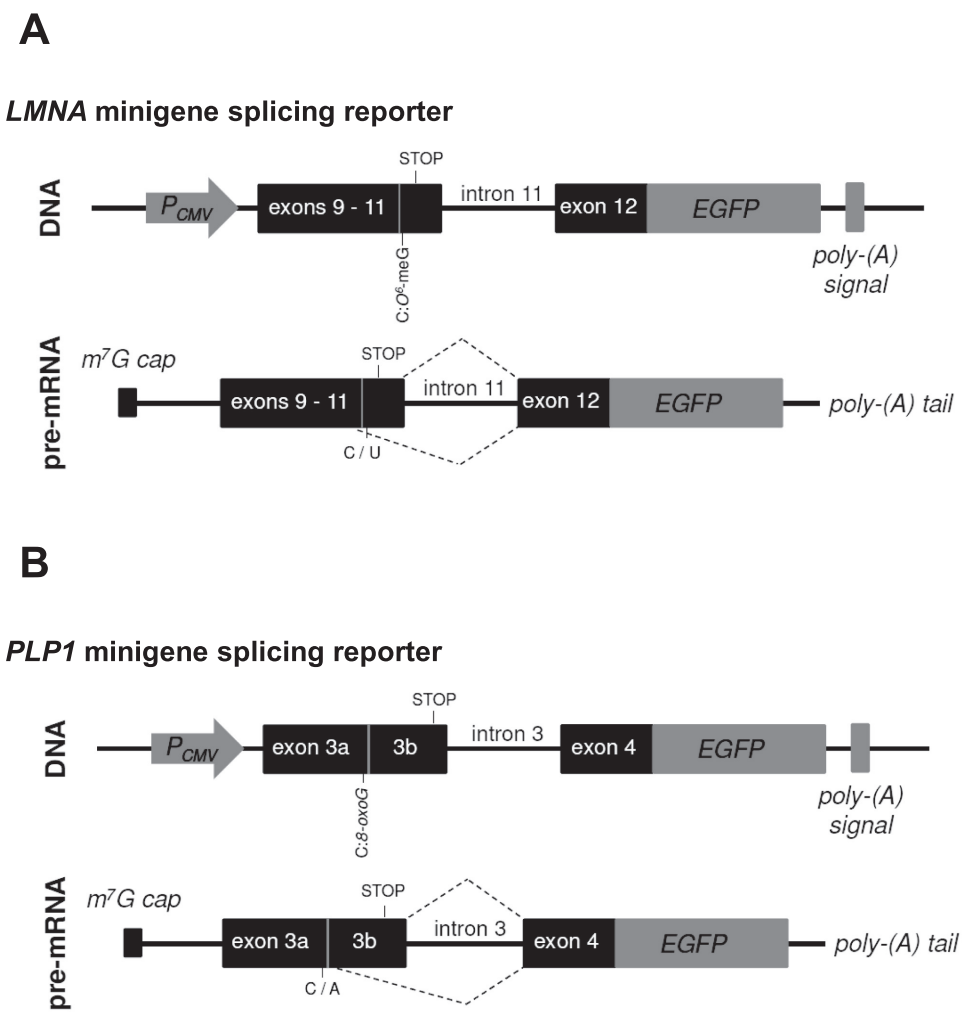

Figure 1. Schematic presentation of the minigene splicing reporters containing site-specific DNA lesions with their resulting pre-mRNA. (**A**) The lamin A (*LMNA*) reporter was based on the region exon 9–11—intron 11—exon 12 of *LMNA*. The nucleotide pair C:O^6-meG indicated corresponds to the sequence of the damaged plasmid. The WT plasmid contains a C:G pair and the mutated a T:A pair in this same position. (**B**) The proteolipid protein 1 (*PLP1*) reporter was based on the region exon 3—intron 4—exon 4 of *PLP1*. The nucleotide pair C:8-oxoG indicated corresponds to the sequence of the damaged plasmid. The WT plasmid contains a C:G pair and the mutated a A:T pair in this same position. The coding sequence for GFP (EGFP) was associated with the minigenes in a manner such that GFP is expressed only if alternative splicing occurs. Transcription of the minigene splicing reporters was under regulation by the human cytomegalovirus immediate early promoter (P_{CMV}) and terminated by the bovine growth hormone polyadenylation [poly-(A)] signal.

Real-time quantitative and reverse-transcription PCR

RNA and cDNA was purified and synthesized as for mRNA sequencing. Real-time qPCR was performed using Maxima SYBR Green qPCR Master Mix (Thermo Fischer scientific) on an Applied Biosystems 7500 Real-time PCR. Quantification of the WT or progerin/Δ150 splicing forms of lamin A was achieved with the fw and rv primer pairs indicated in Figure 3A using ribosomal protein lateral stalk subunit P0 (*RPLP0*) as reference gene. Differences in expression of alternative splicing products were analyzed with two-tailed unpaired *t*-test ($P < 0.05$) using GraphPad Prism 6.0 software.

These same cDNAs were used to detect splicing isoforms transcribed only from the transfected plasmids by RT-PCR. Specific detection of the WT or alternatively spliced forms of LMNA and PLP1, as well as GFP was achieved with the fw and rv primer pairs indicated in Figures 3A and 5A. RT-PCR amplification was performed with the Dream Taq PCR master mix (Thermo Fisher scientific) as follows: 2 min at 95°C, 35 cycles of 30 s at 95°C, 30 s at 54°C and 45 s at 72°C, followed by a final extension of 5 min at 72°C. The PCR products obtained were resolved on a 2% agarose gel. Densitometry was performed using ImageJ. Differences in expression of alternative splicing products were analyzed with two-way anova ($P < 0.05$) using GraphPad Prism 6.0 software. All primer sequences are shown in Supplementary Table S1.

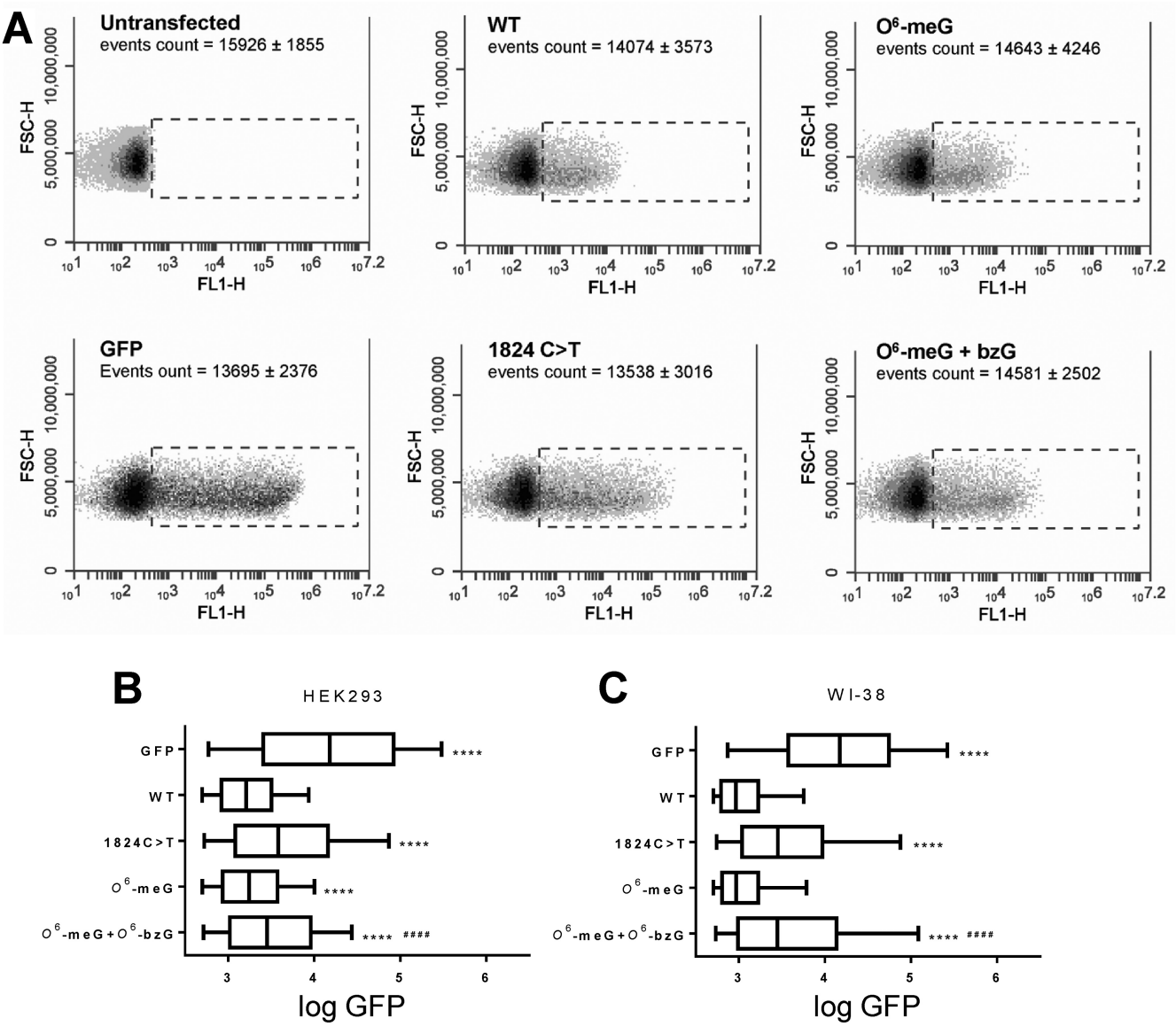

Figure 2. Analysis of splicing based on the GFP fluorescence of cells transfected with the *LMNA* minigene reporter. (**A**) Representative FSC-H/FL1-H scatter plots for HEK293 cells transfected with the different plasmids as indicated (after exclusion of doublets and dead cells) with GFP-positive cells gated relative to untransfected cells. The total counted events for each condition is shown (mean ± SEM, $n = 4$). For representative scatter plots for WI-38 cells see Supplementary Figure S2. (**B** and **C**) Box plots of the distributions (95% CI) of fluorescence intensity in HEK293 and WI-38 cells, respectively. Median $^{****}P < 0.0001$ in comparison to the WT reporter; median $^{\#\#\#\#}P < 0.0001$ in comparison to the O^6-meG reporter, See also Supplementary Table S3.

RESULTS

Construction of minigene splicing reporters

Two minigene splicing reporters containing site-specific DNA lesions were successfully constructed (Figure 1), as confirmed by sequencing and an Fpg nicking assay (Supplementary Figure S1). The lamin A (*LMNA*) reporter (Figure 1A) contained O^6-meG at codon 608, which during transcription should produce RNA containing either the wild-type (WT) *GGC* sequence or the mutated *GGU* due to uridine misincorporation (22,34). This silent mutation at codon 608 in exon 11 (c.1824C>T, p.G608G) increases the usage of a natural splice donor, leading to an in-frame deletion of 150 nucleotides (Δ150) and production of the progerin protein that causes Hutchinson-Gilford progeria syndrome (35,36). The mutation in the *LMNA* 5′ splice site (*CAG'GTGGGC* to *CAG'GTGGGT*) increases the splice-site score from 79.04% to 84.90%.

The proteolipid protein 1 (*PLP1*) reporter (Figure 1B) contained 8-oxoG in codon 116, which during transcription should produce RNA containing either the WT *ACG* sequence or the mutated *AAG* due to adenine misincorporation (21,25). *PLP1* can be spliced into two forms (*PLP1* and *DM20*), due to the alternative use of donor splice sites in exon 3. Mutations that reduce the ratio of *PLP1* to *DM20* (e.g. c.347C>A, p.T116K) result in Pelizaeus-Merzbacher disease, an X-linked leukodystrophy (31,37). The mutation in the *PLP1* 5′ splice site (*ACG'GTAACA* to

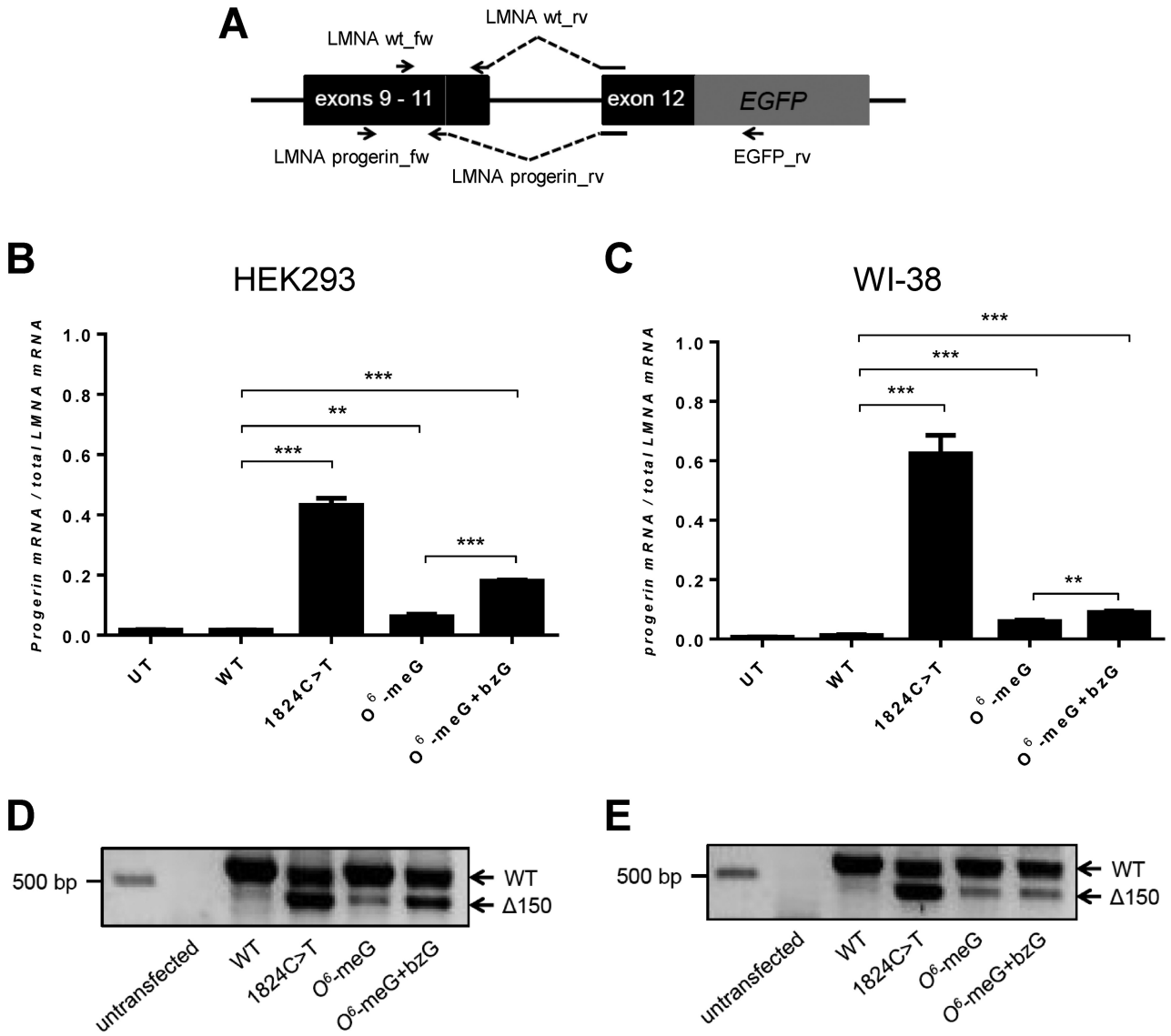

Figure 3. Analysis of splicing in cells transfected with the *LMNA* minigene reporter by qPCR and RT-PCR. (**A**) Schematic illustration of the primers employed. The two LMNA WT and progerin primer pairs were used for qPCR and the LMNA progerin_fw/EGFP_rv pair for RT-PCR. (**B** and **C**) Quantitative analyses of the effects of *LMNA* mRNA on splicing fidelity in HEK293 and WI-38 cells, respectively, presented as the ratio of progerin mRNA / total *LMNA* mRNA (calculated as [R / (1 + R)] where R = progerin / WT *LMNA*) (mean ± SEM, $n = 4$). (**D** and **E**) Agarose gels of RT-PCR products illustrating the effects of TM on splicing fidelity of *LMNA* mRNA in HEK293 and WI-38 cells, respectively. The two splicing forms WT and Δ150 are indicated by arrows. $^{**}P < 0.01$; $^{***}P < 0.001$ in comparison with the WT or O^6-meG reporter.

AAG'GTAACA) elevates the splice-site score from 72.80% to 82.01%.

To allow detection of alternative splicing, the minigenes were associated with an open reading frame GFP (EGFP) in a manner such that GFP is expressed only if alternative splicing occurs (Figure 1). In that event, a STOP codon inserted at the end of the exon containing the donor splicing site disappears from the processed mRNA, allowing for the exon encoding the acceptor splicing site and GFP to be expressed. Along with the plasmid containing a site-specific DNA lesion a control (WT sequence) and mutant (1824C>T or 347C>A) plasmid were synthesized for each reporter. These plasmids contain no known mammalian origin of replication, thereby excluding effects of replication (22).

O^6-meG and 8-oxoG induce transcriptional mutagenesis in mammalian cells

To confirm that O^6-meG and 8-oxoG induce TM, cellular transcripts of these modified reporters were analyzed by sequencing of RT-PCR products. In addition, the impact of DNA repair was assessed by treating HEK293 cells with O^6-benzylguanine (O^6-bzG), an inhibitor of the repair of methylated bases by alkylguanine transferase (AGT) (22,38) or by using primary mouse embryonic fibroblasts (MEFs) deficient in 8-oxoG DNA glycosylase ($OGG1^{-/-}$) (21,39).

In HEK293 cells transfected with the reporter containing O^6-meG uridine misincorporation opposite the lesion was 3.6 ± 1.2% (mean ± SEM, $n = 4$), a value that rose to 20.1 ± 5.6% ($n = 4$, $P < 0.05$) when AGT was inhibited. In the case of MEFs transfected with the reporter containing 8-oxoG adenine misincorporation opposite the lesion in WT and *OGG1*$^{-/-}$ cells was 4.0 ± 1.2% ($n = 4$) and 39.5 ± 2.8% ($n = 4$, $P < 0.0001$), respectively. In HEK293 cells, presence of 8-oxoG resulted in 1.2 ± 0.9% ($n = 3$) TM. No other misincorporations or indels were detected. In agreement with previous studies *in vivo* these data demonstrate that the presence of O^6-meG or 8-oxoG on the transcribed strand of a gene induces TM which, if left unrepaired, can be highly mutagenic (21–23).

Transcriptional mutagenesis reduces splicing fidelity

To determine whether TM induced by O^6-meG or 8-oxoG influenced splicing fidelity, changes in GFP fluorescence were measured by flow cytometry (Figures 2A and 4A; Supplementary Figures S2 and S3). Transfection with the *LMNA* reporter containing O^6-meG resulted in an increase of fluorescence intensity compared to WT in HEK293 cells ($P < 0.0001$), but not in WI-38 fibroblasts (Figure 2B and C). However, when AGT-mediated repair was inhibited, a potent increase in the fluorescence signal was detected in comparison to both the WT and O^6-meG reporters and for both HEK293 and WI-38 cells ($P < 0.0001$), in agreement with the more frequent TM in the presence of impaired AGT. As expected, the fluorescence of both cell types was higher when transfected with the 1824C>T mutant reporter than with the WT reporter ($P < 0.0001$, Figure 2B and C).

The impact of TM on splicing was examined further by quantitative and qualitative PCR analyses using primers specific for each of the splicing forms of *LMNA* mRNA (WT and Δ150/progerin) (Figure 3A). While the qPCR primers also amplified cellular transcripts, the RT-PCR primers were specific for reporter transcripts. Both in the presence (3.6- and 4.8-fold, respectively, $P < 0.01$ and $P < 0.001$) and absence (10- and 7.4-fold, respectively, $P < 0.001$) of active DNA repair, HEK293 and WI-38 cells transfected with the O^6-meG reporter demonstrated higher expression of the Δ150/progerin form than with the WT reporter (Figure 3B and C). Moreover, in both cell types transfected with the O^6-meG this expression was higher in cells with impaired AGT than in cells with active repair ($P < 0.001$ and $P < 0.01$). This quantitative analysis was confirmed by RT-PCR (Figure 3D and E), which also showed that O^6-bzG did not affect splicing of WT *LMNA* (Supplementary Figure S4). As in the case of the fluorescence-based assay, the more extensive alternative splicing in the absence of AGT was in accordance with the higher levels of TM. The observed expression levels of the Δ150/progerin spliced form in the untransfected cells and in the WT *LMNA* transfected cells (Figure 3B and C) are in agreement with previous studies (40).

In the case of the *PLP1* reporter, the effects of TM on splicing fidelity were not as evident, primarily because the two splicing forms PLP1 and DM20 are constitutively expressed, so that such effects will be reflected in the ratio between the two forms. In HEK293 cells and both WT and *OGG1*$^{-/-}$ MEFs transfected with the 347C>A mutant reporter, the increase in fluorescent intensity was only somewhat but nonetheless significantly higher than with the WT reporter ($P < 0.0001$, Figure 4B–D), as was the increase in the fluorescent intensity of HEK293 cells transfected with the 8-oxoG reporter ($P < 0.0001$, Figure 4B). An increase was also observed in *OGG1*$^{-/-}$ MEFs transfected with the 8-oxoG reporter ($P < 0.0001$, Figure 4D) but not in WT MEFs (Figure 4C), in agreement with the impact of *OGG1* status on 8-oxoG-induced TM.

RT-PCR analyses were performed to further confirm the impact of TM on splicing fidelity of *PLP1* (Figure 5A and B). Reproducible quantitative PCR analysis was not successful, although extensive method development was performed. Instead, analysis of band intensities from the PCR of the PLP1 splice variant was used to estimate changes in splicing fidelity due to the presence of 8-oxoG on the transcribed strand in MEFs (Figure 5C). In *OGG1*$^{-/-}$ MEFs a reduction of the PLP1 variant ($P < 0.001$) was observed but not in the WT MEFs, supporting the results based on GFP analysis and confirming the role of DNA repair in reducing TM and thereby maintaining the fidelity of splicing. Together, these results demonstrate that TM in a sequence which regulates splicing can impair splicing fidelity.

DISCUSSION

Here, we show that the presence of unrepaired DNA lesions on the transcribed strand in mammalian cells can cause TM and subsequently reduce the fidelity of mRNA splicing. Employing site-specific mutagenic DNA lesions on the transcribed strand of a reporter vector, we demonstrate that when O^6-meG and 8-oxoG are bypassed by RNA pol II *in vivo* misincorporation opposite the lesion occurs, producing mutant transcripts. The established importance of DNA repair in preventing TM (21,22,24,41,42) was also evident here. In the case of O^6-meG, the frequency of TM in HEK293 increased from 3.6% to 20.1% when AGT was inhibited and the corresponding values for 8-oxoG were from 4.0% to 39.5% when *OGG1* was not expressed in MEFs, clearly showing that if left unrepaired these lesions can be highly mutagenic during transcription. Differences in the sequence flanking the DNA lesion, the relative distance between this lesion and the promoter may explain the small differences in the TM frequency observed here and in previous *in vivo* studies (21–23).

The occurrence, regulation and consequences of transcriptional errors, both spontaneous and due to lesions, have been receiving more and more attention, much due to the information obtainable by next-generation sequencing (11,12,14,42,43). One important aspect for understanding the potential biological significance of transcriptional errors, spontaneous or lesion-induced, is the rate at which such errors occur. In the absence of any known genotoxic insult the transcription error rate in eukaryotic cells is approximately 10^{-5} (14,44,45) and the frequency observed here and by others is three-to-four orders of magnitude higher, depending on the status of DNA repair. If individual transcripts can be translated between 40 and 4000 times (46,47), a single error can result in a considerable amount of erro-

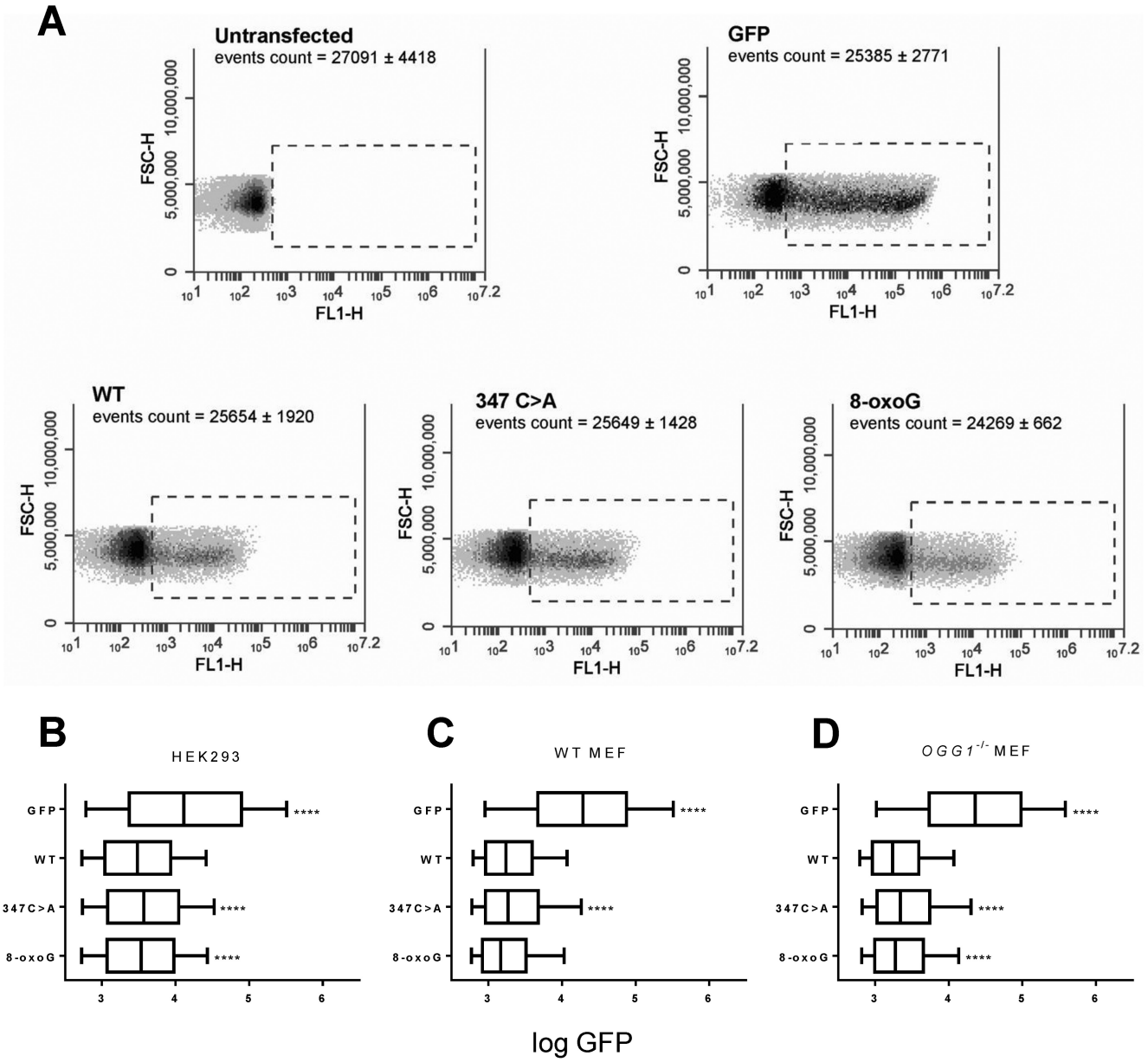

Figure 4. Analysis of splicing based on the GFP fluorescence of cells transfected with the *PLP1* minigene reporter. (**A**) Representative FSC-H/FL1-H scatter plots obtained for HEK293 cells transfected with the different plasmids as indicated (after exclusion of doublets and dead cells) with GFP-positive cells gated relative to untransfected cells. The total counted events for each condition is shown (mean ± SEM, $n = 3$). For representative scatter plots for the WT and *OGG1*$^{-/-}$ MEFs see Supplementary Figure S3. (**B–D**) Box plots of the distributions (95% CI) of the fluorescence intensity in HEK293 cells, WT and *OGG1*$^{-/-}$ MEFs, respectively. Median ****$P < 0.0001$ in comparison with the WT reporter. See also Supplementary Table S3.

neous protein, thereby changing the cellular phenotype. Indeed, since in certain cell types the average level of many mRNAs is less than one per cell (48,49), an error in this molecule may mean that all newly translated protein is abnormal.

All of the relatively few investigations that have examined the biological effects of lesion-induced transcriptional errors in mammalian systems to date reveal that TM can cause phenotypic changes. The TM caused by the presence of 8-oxoG or 5-hydroxyuracil at specific codons of *HRAS* or *KRAS*, respectively, in MEFs lacking *OGG1* or *NEIL1/2* increases the expression levels of mutated and constitutively active Ras proteins, giving rise to sustained downstream oncogenic signaling (21,50). Similarly, the presence of 8-oxoG on the transcribed strand of a gene encoding luciferase in MEFs deficient for *OGG1* impaired the function of this protein due to TM (23). With a fluorescent-based reporter system, Burns and colleagues (22) found that O^6-meG-induced TM in HEK293 cells led to considerable levels of mutated protein with altered function, an effect which was further increased when AGT was impaired. This is in agreement with our observation that during transcription in HEK293 cells with intact repair capacity O^6-meG is more mutagenic than 8-oxoG. This observation might reflect dif-

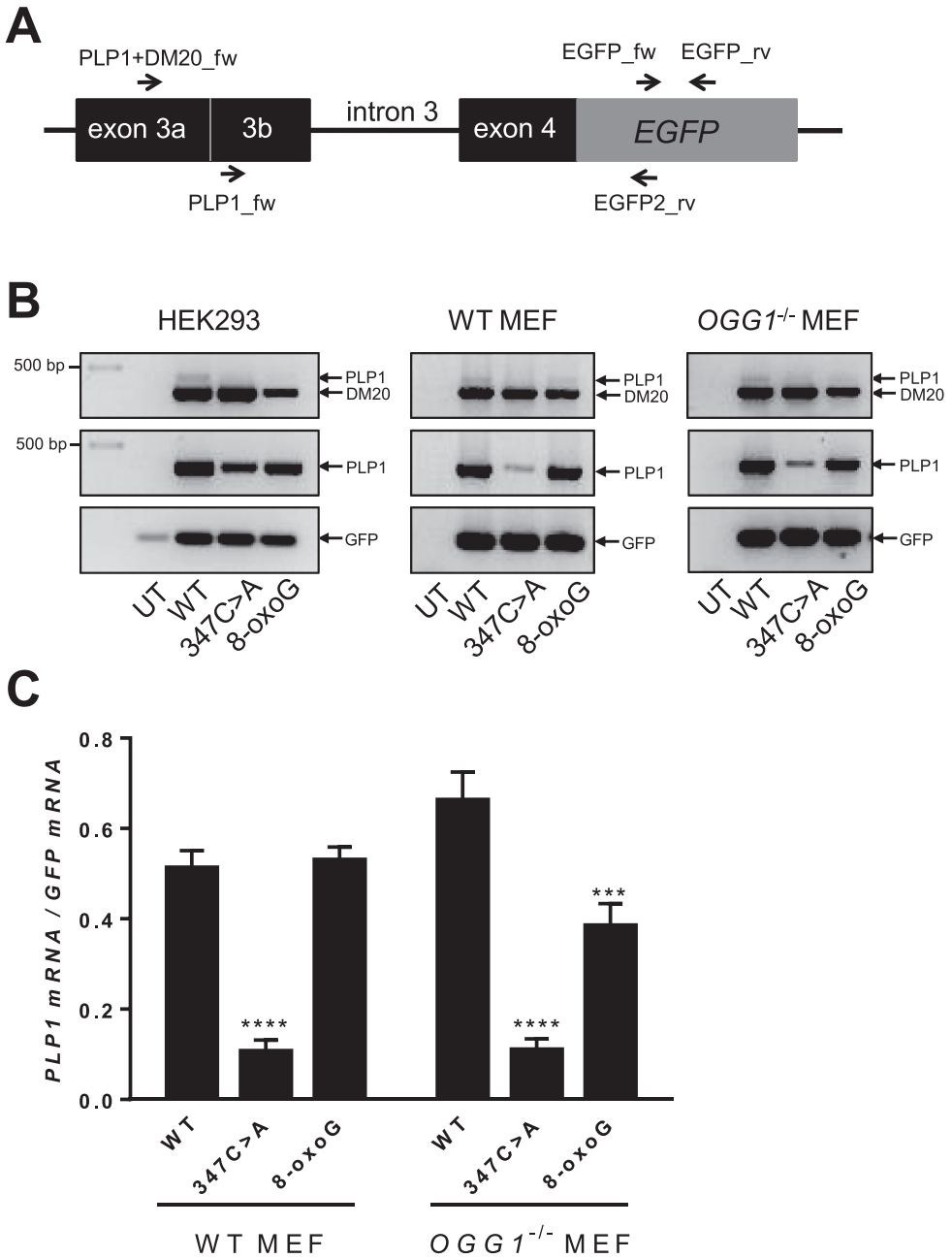

Figure 5. Analysis of splicing in cells transfected with the *PLP1* minigene reporter by RT-PCR. (**A**) Schematic illustration of the primers employed. (**B**) Agarose gel of RT-PCR products showing the effects of TM on splicing fidelity of *PLP1* mRNA in HEK293 cells, WT and *OGG1*$^{-/-}$ MEFs, respectively. The two splicing forms, PLP1 and DM20, and GFP are indicated by arrows. The top gels in B show RT-PCR with primers PLP1+DM20_fw and EGFP2_rv which amplifies both splice forms. Presence of *PLP1* is seen as a weaker band just above the stronger *DM20* band. To facilitate a semi-quantitative analysis, *a PLP1*-specific PCR was performed (middle gels, primers PLP1_fw and EGFP2_rv). Expression of *GFP* is shown in the bottom gels (primers EGFP_fw and EGFP_rv). The faint band observed in the untransfected (UT) lane in HEK293 cells is most likely an unspecific PCR product since any cross contamination would result in PCR product with the other primer pairs as well. (**C**) Densitometric analysis of *PLP1* expression in WT and *OGG1*$^{-/-}$ MEFs using the co-expressed *GFP* as a loading control (mean ± SEM, $n = 3$–4). ***$P < 0.001$; ****$P < 0.0001$ in comparison with the WT reporter.

ferences in the transcriptional fidelity of RNA pol II at these two lesions and/or differences in the kinetics of the repair pathways involved (11).

Genetic variation within splice sites and regulatory sequences frequently results in the aberrant splicing associated with human hereditary diseases and cancer. Single-nucleotide substitutions in the 5′ or the 3′ splice sites are the most common splicing mutations, resulting either in exon skipping, activation of a cryptic splice site or, to a lesser extent, intron retention. The pronounced fidelity of splice-site pairing by the spliceosome suggests that splicing fidelity is limited by the fidelity of transcription (51). Moreover, there is an inverse relationship *in vivo* between the speed of transcription elongation by RNA pol II and splicing efficiency

(13). Clearly, transcription and splicing fidelity are tightly coupled. Here, we demonstrate that induction of TM at a 5′ donor splice site by DNA lesions reduces splicing fidelity, leading to aberrant expression of alternative splicing forms. The impact of TM on splicing fidelity was in general more evident when analyzed on the level of transcripts compared to the GFP-based analysis which also is dependent on translation, protein folding etc., which might affect the quantitative relationship between % TM and GFP readout. This finding extends an earlier study, based on published RNA-seq data from HeLa and Huh7 cells which found enriched transcriptional errors at the 5′ donor site relative to errors at other positions in the human genome, indicating a consequent increase in intron retention during splicing (14). Our results were observed in cells with active DNA repair in response to both lesions employed here, and further emphasized when the protein mainly responsible for repair was inactivated or missing. In agreement with the overall essential role of DNA repair in maintaining genomic integrity, our results show that through its important role in protecting against TM, DNA repair status may also exert a pronounced impact on splicing fidelity.

In conclusion, bypass of mutagenic lesions by RNA pol II, proposed to be the most specific sensor of DNA damage (52), can result in considerable levels of mutant transcripts and the subsequent expression of mutant proteins can lead to phenotypic changes. Here, we show for the first time that TM can reduce splicing fidelity *in vivo*, thereby contributing to the production of altered proteins and/or altering the relative levels of alternatively spliced forms, potentially disturbing cellular homeostasis and triggering numerous diseases. Generation of specific splicing isoforms has recently been found to drive cancer (53,54) and the possibility that such isoforms are expressed as a consequence of lesion-induced TM emphasizes the potential significance of this phenomenon in connection with processes such as carcinogenesis and ageing.

SUPPLEMENTARY DATA

Supplementary Data are available at NAR Online.

ACKNOWLEDGEMENTS

We thank Dr Katarina Johansson for the HEK293 cell line, Dr Pablo Radicella for the primary MEF cells and Dr Maria Eriksson for the tetop-LA^{wt} and tetop-LA^{G608G} plasmids.

Author contributions: J.A.P. and K.D. designed research; J.A.P. and M.E. performed research; J.A.P., M.E., M.B. and K.D. analyzed data; and J.A.P., M.E. and K.D. wrote the paper.

FUNDING

Marie Curie IRG fellowship [2009-256508 to K.D.]; Karolinska Institutet (IMM Junior Faculty fellowship to K.D.); Carl Tryggers Foundation [13-106 to K.D.]; Swedish Research Council VR [621-2012-3686 to K.D.]. Funding for open access charge: Swedish Research Council VR [621-2012-3686].

Conflict of interest statement. None declared.

REFERENCES

1. Sharp,P.A. and Burge,C.B. (1997) Classification of introns: U2-type or U12-type. *Cell*, **91**, 875–879.
2. Keren,H., Lev-Maor,G. and Ast,G. (2010) Alternative splicing and evolution: diversification, exon definition and function. *Nat. Rev. Genet.*, **11**, 345–355.
3. Nilsen,T.W. and Graveley,B.R. (2010) Expansion of the eukaryotic proteome by alternative splicing. *Nature*, **463**, 457–463.
4. Merkin,J., Russell,C., Chen,P. and Burge,C.B. (2012) Evolutionary dynamics of gene and isoform regulation in Mammalian tissues. *Science*, **338**, 1593–1599.
5. Barbosa-Morais,N.L., Irimia,M., Pan,Q., Xiong,H.Y., Gueroussov,S., Lee,L.J., Slobodeniuc,V., Kutter,C., Watt,S., Colak,R. *et al.* (2012) The evolutionary landscape of alternative splicing in vertebrate species. *Science*, **338**, 1587–1593.
6. Ward,A.J. and Cooper,T.A. (2010) The pathobiology of splicing. *J. Pathol.*, **220**, 152–163.
7. Singh,R.K. and Cooper,T.A. (2012) Pre-mRNA splicing in disease and therapeutics. *Trends Mol. Med.*, **18**, 472–482.
8. Kornberg,R.D. (2007) The molecular basis of eukaryotic transcription. *Proc. Natl. Acad. Sci. U.S.A.*, **104**, 12955–12961.
9. Nouspikel,T. and Hanawalt,P.C. (2002) DNA repair in terminally differentiated cells. *DNA Repair (Amst.)*, **1**, 59–75.
10. Yao,G. (2014) Modelling mammalian cellular quiescence. *Interface Focus*, **4**, 20130074.
11. Xu,L., Wang,W., Chong,J., Shin,J.H., Xu,J. and Wang,D. (2015) RNA polymerase II transcriptional fidelity control and its functional interplay with DNA modifications. *Crit. Rev. Biochem. Mol. Biol.*, **50**, 503–519.
12. Vermulst,M., Denney,A.S., Lang,M.J., Hung,C.W., Moore,S., Moseley,M.A., Thompson,J.W., Madden,V., Gauer,J., Wolfe,K.J. *et al.* (2015) Transcription errors induce proteotoxic stress and shorten cellular lifespan. *Nat. Commun.*, **6**, 8065.
13. Braberg,H., Jin,H., Moehle,E.A., Chan,Y.A., Wang,S., Shales,M., Benschop,J.J., Morris,J.H., Qiu,C., Hu,F. *et al.* (2013) From structure to systems: high-resolution, quantitative genetic analysis of RNA polymerase II. *Cell*, **154**, 775–788.
14. Carey,L.B. (2015) RNA polymerase errors cause splicing defects and can be regulated by differential expression of RNA polymerase subunits. *Elife*, **4**, e09945.
15. Hanawalt,P.C. and Spivak,G. (2008) Transcription-coupled DNA repair: two decades of progress and surprises. *Nat. Rev. Mol. Cell. Biol.*, **9**, 958–970.
16. Saxowsky,T.T. and Doetsch,P.W. (2006) RNA polymerase encounters with DNA damage: transcription-coupled repair or transcriptional mutagenesis? *Chem. Rev.*, **106**, 474–488.
17. Dreij,K., Burns,J.A., Dimitri,A., Nirenstein,L., Noujnykh,T. and Scicchitano,D.A. (2010) In: Geacintov,NE and Broyde,S (eds). *The Chemical Biology of DNA damage*. Wiley-VCH Verlag, Weinheim, pp. 399–437.
18. Laine,J.P. and Egly,J.M. (2006) When transcription and repair meet: a complex system. *Trends Genet.*, **22**, 430–436.
19. Walmacq,C., Cheung,A.C., Kireeva,M.L., Lubkowska,L., Ye,C., Gotte,D., Strathern,J.N., Carell,T., Cramer,P. and Kashlev,M. (2012) Mechanism of translesion transcription by RNA polymerase II and its role in cellular resistance to DNA damage. *Mol. Cell*, **46**, 18–29.
20. Li,W., Selvam,K., Ko,T. and Li,S. (2014) Transcription bypass of DNA lesions enhances cell survival but attenuates transcription coupled DNA repair. *Nucleic Acids Res.*, **42**, 13242–13253.
21. Saxowsky,T.T., Meadows,K.L., Klungland,A. and Doetsch,P.W. (2008) 8-Oxoguanine-mediated transcriptional mutagenesis causes Ras activation in mammalian cells. *Proc. Natl. Acad. Sci. U.S.A.*, **105**, 18877–18882.
22. Burns,J.A., Dreij,K., Cartularo,L. and Scicchitano,D.A. (2010) O6-methylguanine induces altered proteins at the level of transcription in human cells. *Nucleic Acids Res.*, **38**, 8178–8187.
23. Bregeon,D., Peignon,P.A. and Sarasin,A. (2009) Transcriptional mutagenesis induced by 8-oxoguanine in mammalian cells. *PLoS Genet.*, **5**, e1000577.

24. Viswanathan,A., You,H.J. and Doetsch,P.W. (1999) Phenotypic change caused by transcriptional bypass of uracil in nondividing cells. *Science*, **284**, 159–162.
25. Bregeon,D., Doddridge,Z.A., You,H.J., Weiss,B. and Doetsch,P.W. (2003) Transcriptional mutagenesis induced by uracil and 8-oxoguanine in Escherichia coli. *Mol. Cell*, **12**, 959–970.
26. Bregeon,D. and Doetsch,P.W. (2011) Transcriptional mutagenesis: causes and involvement in tumour development. *Nat. Rev. Cancer*, **11**, 218–227.
27. Taddei,F., Hayakawa,H., Bouton,M., Cirinesi,A., Matic,I., Sekiguchi,M. and Radman,M. (1997) Counteraction by MutT protein of transcriptional errors caused by oxidative damage. *Science*, **278**, 128–130.
28. Bregeon,D. and Doetsch,P.W. (2004) Reliable method for generating double-stranded DNA vectors containing site-specific base modifications. *Biotechniques*, **37**, 760–766.
29. Desviat,L.R., Perez,B. and Ugarte,M. (2012) Minigenes to confirm exon skipping mutations. *Methods Mol. Biol.*, **867**, 37–47.
30. Scaffidi,P. and Misteli,T. (2006) Lamin A-dependent nuclear defects in human aging. *Science*, **312**, 1059–1063.
31. Hobson,G.M., Huang,Z., Sperle,K., Sistermans,E., Rogan,P.K., Garbern,J.Y., Kolodny,E., Naidu,S. and Cambi,F. (2006) Splice-site contribution in alternative splicing of PLP1 and DM20: molecular studies in oligodendrocytes. *Hum. Mutat.*, **27**, 69–77.
32. Ye,S., Dhillon,S., Ke,X., Collins,A.R. and Day,I.N. (2001) An efficient procedure for genotyping single nucleotide polymorphisms. *Nucleic Acids Res.*, **29**, E88–88.
33. Huber,P.J. (1967), *Proceedings of the Fifth Berkeley Symposium on Mathematical Statistics and Probability*. University of California Press, Berkeley, Vol. **1**, pp. 221–233.
34. Dimitri,A., Burns,J.A., Broyde,S. and Scicchitano,D.A. (2008) Transcription elongation past O6-methylguanine by human RNA polymerase II and bacteriophage T7 RNA polymerase. *Nucleic Acids Res.*, **36**, 6459–6471.
35. De Sandre-Giovannoli,A., Bernard,R., Cau,P., Navarro,C., Amiel,J., Boccaccio,I., Lyonnet,S., Stewart,C.L., Munnich,A., Le Merrer,M. *et al.* (2003) Lamin a truncation in Hutchinson-Gilford progeria. *Science*, **300**, 2055.
36. Eriksson,M., Brown,W.T., Gordon,L.B., Glynn,M.W., Singer,J., Scott,L., Erdos,M.R., Robbins,C.M., Moses,T.Y., Berglund,P. *et al.* (2003) Recurrent de novo point mutations in lamin A cause Hutchinson-Gilford progeria syndrome. *Nature*, **423**, 293–298.
37. Nance,M.A., Boyadjiev,S., Pratt,V.M., Taylor,S., Hodes,M.E. and Dlouhy,S.R. (1996) Adult-onset neurodegenerative disorder due to proteolipid protein gene mutation in the mother of a man with Pelizaeus-Merzbacher disease. *Neurology*, **47**, 1333–1335.
38. Dolan,M.E., Pegg,A.E., Moschel,R.C. and Grindey,G.B. (1993) Effect of O6-benzylguanine on the sensitivity of human colon tumor xenografts to 1,3-bis (2-chloroethyl)-1-nitrosourea (BCNU). *Biochem. Pharmacol.*, **46**, 285–290.
39. Klungland,A., Rosewell,I., Hollenbach,S., Larsen,E., Daly,G., Epe,B., Seeberg,E., Lindahl,T. and Barnes,D.E. (1999) Accumulation of premutagenic DNA lesions in mice defective in removal of oxidative base damage. *Proc. Natl. Acad. Sci. U.S.A.*, **96**, 13300–13305.
40. Cao,K., Blair,C.D., Faddah,D.A., Kieckhaefer,J.E., Olive,M., Erdos,M.R., Nabel,E.G. and Collins,F.S. (2011) Progerin and telomere dysfunction collaborate to trigger cellular senescence in normal human fibroblasts. *J. Clin. Invest.*, **121**, 2833–2844.
41. Nadkarni,A., Burns,J.A., Gandolfi,A., Chowdhury,M.A., Cartularo,L., Berens,C., Geacintov,N.E. and Scicchitano,D.A. (2016) Nucleotide excision repair and transcription-coupled DNA repair abrogate the impact of DNA damage on transcription. *J. Biol. Chem.*, **291**, 848–861.
42. Nagel,Z.D., Margulies,C.M., Chaim,I.A., McRee,S.K., Mazzucato,P., Ahmad,A., Abo,R.P., Butty,V.L., Forget,A.L. and Samson,L.D. (2014) Multiplexed DNA repair assays for multiple lesions and multiple doses via transcription inhibition and transcriptional mutagenesis. *Proc. Natl. Acad. Sci. U.S.A.*, **111**, E1823–E1832.
43. Acevedo,A., Brodsky,L. and Andino,R. (2014) Mutational and fitness landscapes of an RNA virus revealed through population sequencing. *Nature*, **505**, 686–690.
44. Gout,J.F., Thomas,W.K., Smith,Z., Okamoto,K. and Lynch,M. (2013) Large-scale detection of in vivo transcription errors. *Proc. Natl. Acad. Sci. U.S.A.*, **110**, 18584–18589.
45. van Dijk,D., Dhar,R., Missarova,A.M., Espinar,L., Blevins,W.R., Lehner,B. and Carey,L.B. (2015) Slow-growing cells within isogenic populations have increased RNA polymerase error rates and DNA damage. *Nat. Commun.*, **6**, 7972.
46. Golding,I., Paulsson,J., Zawilski,S.M. and Cox,E.C. (2005) Real-time kinetics of gene activity in individual bacteria. *Cell*, **123**, 1025–1036.
47. Schwanhausser,B., Busse,D., Li,N., Dittmar,G., Schuchhardt,J., Wolf,J., Chen,W. and Selbach,M. (2011) Global quantification of mammalian gene expression control. *Nature*, **473**, 337–342.
48. Pelechano,V., Chavez,S. and Perez-Ortin,J.E. (2010) A complete set of nascent transcription rates for yeast genes. *PLoS One*, **5**, e15442.
49. Islam,S., Kjallquist,U., Moliner,A., Zajac,P., Fan,J.B., Lonnerberg,P. and Linnarsson,S. (2011) Characterization of the single-cell transcriptional landscape by highly multiplex RNA-seq. *Genome Res.*, **21**, 1160–1167.
50. Petrova,L., Gran,C., Bjoras,M. and Doetsch,P.W. (2016) Efficient and reliable production of vectors for the study of the repair, mutagenesis, and phenotypic consequences of defined DNA damage lesions in mammalian cells. *PLoS One*, **11**, e0158581.
51. Fox-Walsh,K.L. and Hertel,K.J. (2009) Splice-site pairing is an intrinsically high fidelity process. *Proc. Natl. Acad. Sci. U.S.A.*, **106**, 1766–1771.
52. Lindsey-Boltz,L.A. and Sancar,A. (2007) RNA polymerase: the most specific damage recognition protein in cellular responses to DNA damage? *Proc. Natl. Acad. Sci. U.S.A.*, **104**, 13213–13214.
53. Sveen,A., Kilpinen,S., Ruusulehto,A., Lothe,R.A. and Skotheim,R.I. (2016) Aberrant RNA splicing in cancer; expression changes and driver mutations of splicing factor genes. *Oncogene*, **35**, 2413–2427.
54. Zheng,S., Kim,H. and Verhaak,R.G. (2014) Silent mutations make some noise. *Cell*, **156**, 1129–1131.